Journal of Innovative Optical Health Sciences
Vol. 3, No. 3 (2010) 183–188

DOI: 10.1142/S1793545810001064

ASSESSMENT OF OPTICAL CLEARING AGENTS USING REFLECTANCE-MODE CONFOCAL SCANNING LASER MICROSCOPY

RAVIKANT SAMATHAM, KEVIN G. PHILLIPS and
STEVEN L. JACQUES*
Departments of Dermatology and Biomedical Engineering
Oregon Health and Science University
3303 SW Bond Avenue, Portland, OR 97239, USA
**jacquess@ohsu.edu*

The mechanism of action of clearing agents to improve optical imaging of mouse skin during reflectance-mode confocal microscopy was tested. The dermal side of excised dorsal mouse skin was exposed for one hour to saline, glycerin, or 80% DMSO, then the clearing agent was removed and the dermis placed against a glass cover slip through which a confocal microscope measured reflectance at 488 nm wavelength. An untreated control was also measured. The axial attenuation of reflectance signal, $R(z_f)$ versus increasing depth of focus z_f behaved as $R = \rho \exp(-\mu z_f 2G)$, where ρ is tissue reflectivity and μ is attenuation [cm^{-1}]. The factor $2G$ accounts for the in/out path of photons, and the numerical aperture of the lens. The ρ, μ data were mapped to values of scattering coefficient (μ_s [cm^{-1}]) and anisotropy of scattering (g). Images showed that glycerin significantly increased the g of dermis from about 0.7 to about 0.99, with little change in the μ_s of dermis at about 300 cm^{-1}. DMSO and saline had only slight and inconsistent effects on g and μ_s.

Keywords: Optical properties; skin; anisotropy.

1. Introduction

Clearing agents offer a means of clarifying a tissue by modifying the optical scattering properties, which allows better penetration of light into the tissue. This clarification is achieved by applying a clearing agent like glycerin to the skin, which penetrates into the skin. The glycerin entering the dermis is expected to increase the refractive index of the tissue as well as to osmotically withdraw water from the dermal collagen fibers, thereby yielding a less scattering tissue. In previous work, we have used reflectance mode confocal microscopy to image the superficial layers of mouse skin to investigate onset of melanoma in murine cancer models,[1] genetic changes in skin,[2] and epidermal thickening due to keratinocyte proliferation.[3]

In this report, confocal reflectance imaging is used to specify tissue optical scattering properties of skin dermis exposed to clearing agents. In such imaging, the initial magnitude and attenuation of reflectance, as the focus is scanned into the tissue, provides information about the optical properties of scattering coefficient (μ_s [cm^{-1}]) and anisotropy of scattering (g). The effects of clearing agents (saline, 80% DMSO, pure glycerin) on the μ_s and g of scattering at 488 nm wavelength of mouse dermis are presented.

2. Materials and Methods

Three 14-week-old mice on a C57/Black genetic background were euthanized and from each mouse four skin samples from depilated regions of the back were freshly excised and the dermal side of each specimen was scraped clean of any muscle and subcutaneous fat. This dermal surface was immediately placed in a shallow pool of either saline, glycerin (Fischer Scientific, 99.9% pure), or DMSO (Fischer Scientific) diluted by water to an 80% solution,[4] held within a small Petri dish. The clearing agents were allowed to permeate the skin tissues for one hour,[5] then blotted dry with a medical Q-tip. Samples were then placed against a glass cover slip that was positioned on the optical stage of an inverted reflectance-mode confocal scanning laser microscope (rCSLM), using water to couple the lens to the glass cover slip. One sample was kept moist but not immersed in any fluid, then measured, which served as a control. A total of 12 samples (3 mice × 4 samples) were imaged before and after treatment. All animal studies were approved by the Oregon Health and Science University Institutional Animal Care and Use Committee.

2.1. *Imaging system*

The rCSLM microscope (see Fig. 1) was built in our laboratory using a 60X water dipping objective lens (NA = 0.90, LUMPlanFL, Olympus America, Melville, New York) in an inverted configuration. Tissues were illuminated by an argon ion laser (λ = 488 nm wavelength) with an output of 100 mW. Axial translation of the focus was achieved by translating the sample using a motorized scanning stage (LS50A, Applied Scientific Instrumentation, Eugene, Oregon). Lateral scanning at each depth of focus was implemented by x- and y-galvo scanning mirrors (RS-15, Nutfield Technology Inc., Windham, New Hampshire). The z-axis stage stepped through 80–120 1-μm steps, and the x- and y-axis scanning mirrors captured a 512×546 pixel image at each depth of focus. The pixel size was $0.42\,\mu\text{m} \times 0.42\,\mu\text{m}$. The detection arm of the rCSLM was a lens/pinhole/Photomultiplier-tube assembly (PMT: 5773-01, Hamamatsu Photonics, Japan). Scanning and detection were controlled by a data acquisition board (6062E, National Instruments, Austin, TX) and custom software developed using Labview$^{\text{TM}}$. Image reconstruction and analysis were done using MATLAB (The Mathworks Inc., Natick, Massachusetts).

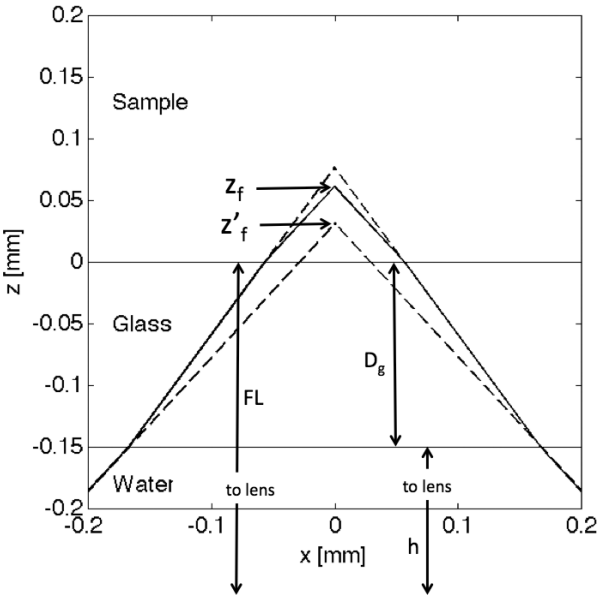

Fig. 1. The confocal microscope operates in inverted mode, delivering light from below from the lens through water and a glass cover slip into the sample. The relationship between the true position of the focus (z_f) (solid line) and the apparent position of the focus, $z'_f = FL - (h + D_g)$ (dashed line), where h is the distance between the lens and the glass/sample interface and D_g is the thickness of the glass cover slip, is described as $z_f = z'_f \partial z_f / \partial z'_f$, where $\partial z_f / \partial z'_f$ equals 1.000, 1.055, 1.161 and 1.187 for water (saline), skin (dermis), 80%DMSO, and glycerin, respectively, at 488 nm wavelength. (Refractive indices are $n_{\text{water}} \approx 1.33$, $n_{\text{dermis}} \approx 1.38$, $n_{80\%\text{DMSO}} \approx 1.45$, $n_{\text{glycerin}} \approx 1.47$).

Figure 1 illustrates the penetration of light into a sample from below in the inverted microscope. Controlling the height of the sample stage controlled the lens/glass-cover slip distance (h), which in turn controlled the apparent depth of the focus, z'_f. As light moved through the lens/water/glass-slide/tissue interfaces, refraction occurred that affected the true depth of the focus within the tissue. In Fig. 1, the apparent depth z'_f is shown by the dashed lines, while the true focus z_f is shown by the solid lines. The change in z_f relative to a change in z'_f was determined by ray tracing. The refractive index values of saline, skin (dermis), 80% DMSO,[6] and glycerol[7] were 1.33, 1.38, 1.45 and 1.47, respectively, which resulted in $\partial z_f / \partial z'_f$ to equal 1.00, 1.055, 1.161 and 1.187, respectively. The true value of the focus was calculated:

$$z_f = \frac{\partial z_f}{\partial z'_f}(FL - (h + D_g)), \tag{1}$$

where h was the lens-glass distance, D_g was the thickness of the glass, and FL was the focal length

of the lens. The refraction also influenced the apparent numerical aperture of the objective lens, in other words, changed the solid angle of collection of backscattered light. This small correction was also included in the calculation of G [see Eq. (3)]. In summary, the refractive index of the sample was considered in the calculations.

2.2. *Image processing*

The rCSLM system stored a reflectance signal from the PMT, V [Volts], from the different tissue samples in a three dimensional array, $V(x, y, z'_f)$. Here x and y corresponded to transverse directions, while z'_f corresponded to the apparent axial distance of the focus within the tissue prior to correction for the refractive index of the sample. The average axial reflectance profile for a region of interest on the skin was calculated:

$$R(z'_f) = \frac{1}{CALIB}\frac{1}{N}\sum_{i=1}^{N} V(x_i, y_i, z'_f), \qquad (2)$$

averaging $N = 100$ voxels within 10×10 x, y voxels for each of 100 z-axis depths. This region of interest corresponded to a $4\,\mu\text{m} \times 4\,\mu\text{m} \times 100\,\mu\text{m}$ volume. After correcting for any refraction, the $R(z_f)$ signal decayed exponentially versus the true depth of focus z_f, characterized by a local reflectivity ρ and an attenuation coefficient μ [cm^{-1}]:

$$R(z_f) = \rho e^{-\mu z_f}. \qquad (3)$$

The optical properties were extracted from $R(z_f)$ by mapping the ρ and μ into the scattering coefficient, μ_s [cm^{-1}], and anisotropy of scattering, g [dimensionless], using the expressions[2,8,9]:

$$\begin{aligned} \mu &= a_g \mu_s 2G, \\ \rho &= \mu_s \Delta z b_g, \end{aligned} \qquad (4)$$

where a_g is a factor that mitigates the effect of scattering to prevent transmission of photons to/from the focus; a_g depends on g and decreases to zero as g approaches 1. The factor $2G$ multiplies the depth of focus, z_f [cm], to yield the round-trip photon pathlength in the tissue, in which G depends on the effective numerical aperture (NA_{eff}) of the objective lens as light enters the sample. The calculation of G considered the refractive index of each type of clearing agent at the glass/sample interface. The axial extent of the focus is $\Delta z \approx 1.4\lambda/(NA_{\text{eff}})^2$, and the product $\mu_s \Delta z$ is the fraction of light reaching the focus that is scattered within the focus. A fraction b_g of this scattered light is backscattered within the solid angle of collection of the objective lens, where b_g depends on g and the NA of the lens. The calculation of b_g used the NA_{eff} appropriate for each type of clearing agent. Table 1 summarizes the values of parameters used in Eq. (4) as a function of the clearing agent.

A calibration constant (CALIB [Volts^{-1}]) adjusted the magnitude of the raw data such that the resulting mean value of g for the control and saline-soaked samples matched the g of previous experiments, $g \approx 0.7$ for skin at 488 nm. In previous experiments, 100-nm-dia. polysytrene microspheres in soft agar gel at a 1% volume fraction were used to calibrate the system. The value of CALIB was determined by measurements of a phantom consisting of polystyrene microspheres in water (yields $\mu_s = 57\,\text{cm}^{-1}$, $g = 0.112$ at 488 nm wavelength). The μ value did not need adjustment since it is a relative measurement; μ was in agreement with previous experiments.

3. Results

The skin samples were placed on a white surface with a black line, such that the visibility of the line beneath the samples could be photographed. Figure 2 shows representative samples for the four tested conditions (control, and one-hour exposure to saline, DMSO, glycerin) before and after the exposure to clearing agent. The glycerin-exposed

Table 1. The refractive index of the clearing agent on the glass/sample interface affects the relationship ($\partial z_f/\partial z'_f$) between the true focus (z_f) and apparent focus (z'_f).

Sample	n	$\partial z_f/\partial z'_f$	NA	L_f	G	b_g	a_g
Water	1.33	1.000	0.900	8.43e-05	1.107	0.015	0.944
Skin (dermis)	1.38	1.055	0.867	9.08e-05	1.096	0.014	0.944
80%DMSO	1.45	1.161	0.826	1.00e-04	1.085	0.012	0.944
Glycerin	1.47	1.187	0.814	1.03e-04	1.082	0.012	0.944

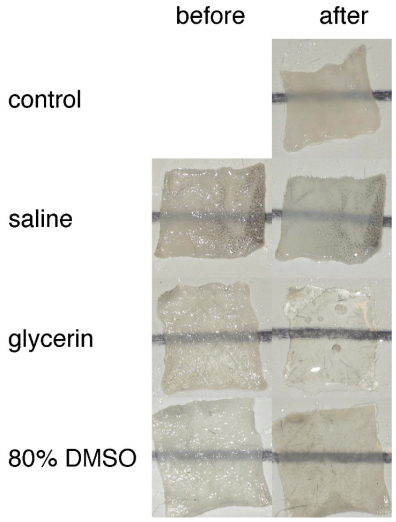

Fig. 2. Images of skin tissue showing control sample, and before and after one-hour treatment with saline, glycerin or 80% DMSO. The glycerin sample is strongly cleared. The 80% DMSO sample is partially cleared.

sample has significantly clarified. The other samples showed little change.

Figure 3 shows sagittal views of the skin samples, $R(z'_f, x)$ at y, expressed as the raw data $\log_{10}$(Detector voltage). The control, saline- and DMSO-exposed samples presented stronger reflectivity than the glycerin-exposed samples that presented very low reflectivity.

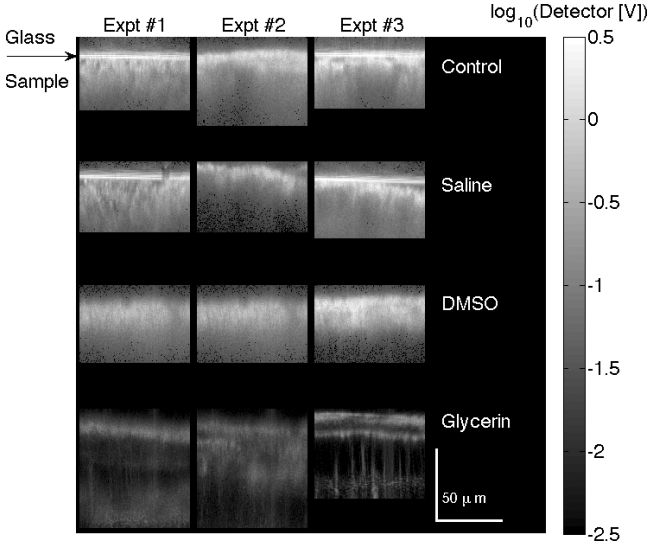

Fig. 3. Sagittal views of the skin samples from three mice, showing the reflected signal, $R(z'_f, x)$, in the original lab units of detector volts $[V]$ acquired by the microscope as a function of the apparent depth of focus (z'_f) and lateral position (x). The color bar indicates the $\log_{10}$(Detector $[V]$). The top bright surface is the glass/sample interface (arrow). The signal decays as the microscope scans deeper into the tissue. The glycerin image is darker, indicating less reflectance from the glass/glycerin interface and from within the skin sample.

Figure 4(a) shows the axial profiles of the detected reflectance, $R(z_f)$ at x, y, along with the exponential fits using Eq. (3), which are shown as dashed lines where the black dot indicates the value of ρ and the slope indicates the value of μ. The glycerin shows a much lower reflectivity ρ while the attenuation μ for all samples is similar. Figure 3(b) plots the μ vs ρ on a loglog scale, and superimposes the calibration grid of μ_s vs g based on Eq. (4). The plot suggests that glycerin has a greatly increased anisotropy of scattering (g) while its scattering coefficient (μ_s) is only slightly affected. The DMSO and saline may have had some slight effects on dermal properties, but the effects were not reliably reproducible in these experiments.

4. Discussion

In these preliminary experiments, there was significant variability in the data. Nevertheless, there was a clear indication of glycerin increasing the anisotropy (g) of scattering, while having little effect on the scattering coefficient itself (μ_s). To explain the optical clearing effect of glycerin on dermal scattering, the matching of refractive index between collagen fibers and surrounding medium seems the obvious explanation. However, this hypothesis can be tested.

Consider a solution of microspheres (diameter $D_o = 0.250\,\mu$m, volume fraction $v_f = 0.12$, $n_{\text{med}} = 1.33$, $n_{\text{par}} = 1.50$) that mimics the observed optical properties of skin ($\mu_s \approx 300\,\text{cm}^{-1}$, $g \approx 0.70$, at 488-nm wavelength) when using Mie theory. Now increase the refractive index of the medium, n_{med} from 1.33 to 1.47 in steps of 0.02. Also increase the size of the particle from D_o to $2D_o$, $4D_o$ and $8D_o$. For each case, use Mie theory to calculate μ_s and g, then Eq. (4) to calculate μ and ρ. Figure 5 shows the result. A bold-line grid is shown which indicates how the parameters μ, ρ and μ_s, g would vary as n_{med} and diameter are increased. The grid indicates that increasing n_{med} will cause μ_s to drop, but not strongly affect g. In contrast, increasing the particle diameter will cause g to increase but cause only a slight drop in μ_s.

The details of this latter effect on μ_s as n_{med} increases depends on the degree to which the

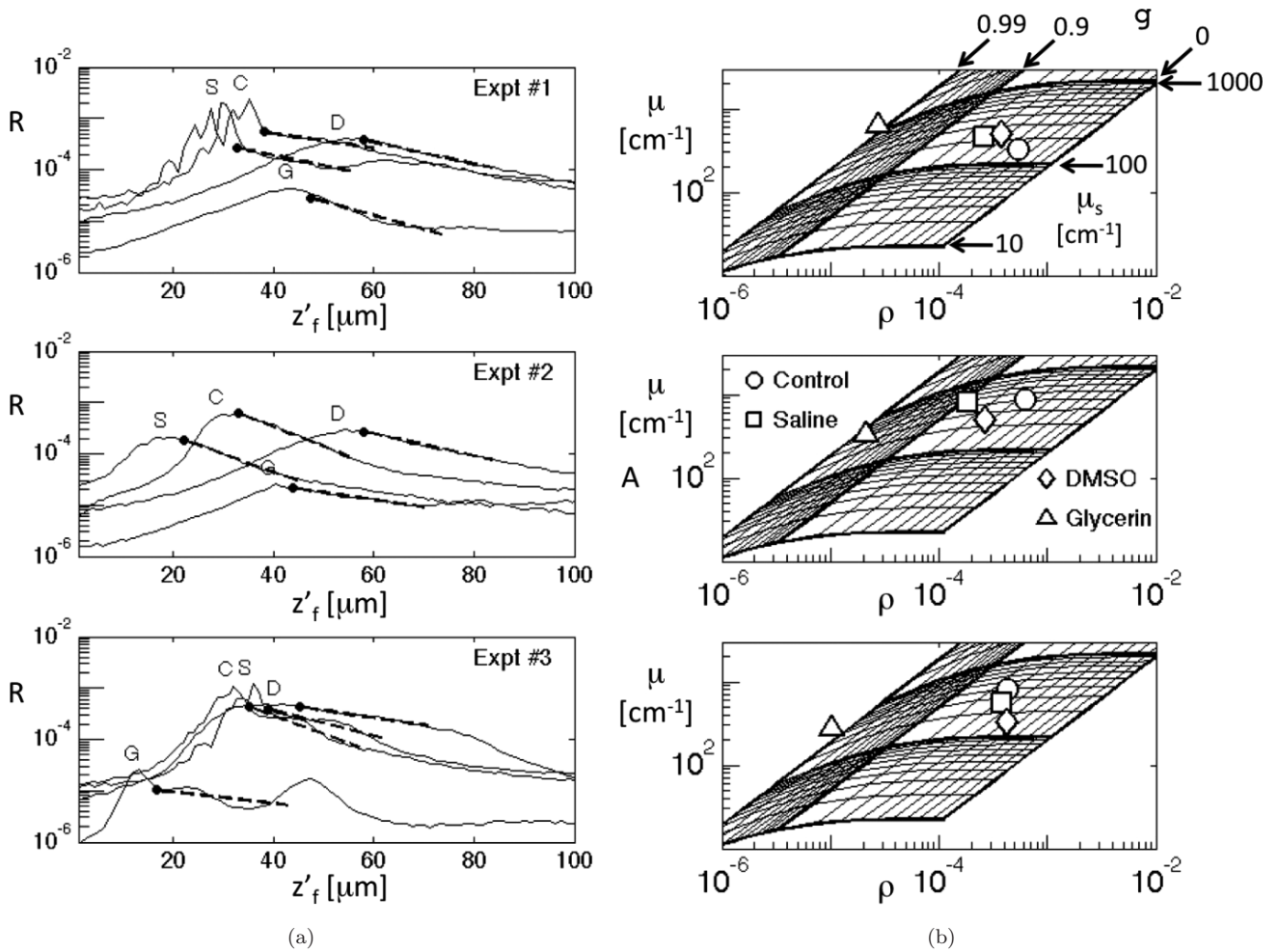

(a) (b)

Fig. 4. The experimental data, attenuation (μ) versus reflectivity (ρ), for three mice (labeled #1, #2 and #3) for the four conditions of control, and after one-hour exposure to saline, glycerin or 80% DMSO. (a) Axial profiles. Dashed lines show region of fitting to specify $\mu s\rho$. The black dot indicates ρ and the slope indicates μ. (b) Plots of μ vs ρ, with analysis grid μ_s, g superimposed. The glycerin caused a significant increase in g but little obvious change in μ_s. DMSO and saline may have had some slight effects, which were not reliably reproducible in these experiments.

particle refractive index, n_{par}, changes as it swells due to exposure to a clearing agent. In Fig. 5, the n_{par} was allowed to approach the refractive index of the surrounding n_{med} proportionately as its volume increased, as if the particle were becoming swollen by the clearing agent. But even if the n_{par} were kept constant during the change in particle diameter, a similar bold-line grid still occurs. The basic conclusion is that only a change in particle size can explain the significant drop in ρ and with little change μ, corresponding to an increase in anisotropy g while μ_s is relatively stable.

In conclusion, this report describes the reflected light collected by a confocal microscope as the focus is scanned into freshly excised mouse dermis, for dermal samples that were exposed for one hour to saline, DMSO and glycerin, or not exposed as a control. The axial profiles of reflectance, $R(z_f)$, were analyzed by Eq. (3) to yield the attenuation μ and reflectivity ρ, and by Eq. (4) to yield the scattering coefficient μ_s and anisotropy of scattering g. The glycerin sample showed a strong drop in ρ, corresponding to a significant increase in g, with little effect on μ_s. The clearing effect of glycerin appears to be due to reducing the angular deviation of scattering, rather than reducing the frequency of scattering. Simulations using Mie theory suggest that this increase in g with minor change in μ_s must involve an increase in the size of the scattering particles, which likely means a swelling of collagen fibers in dermis.

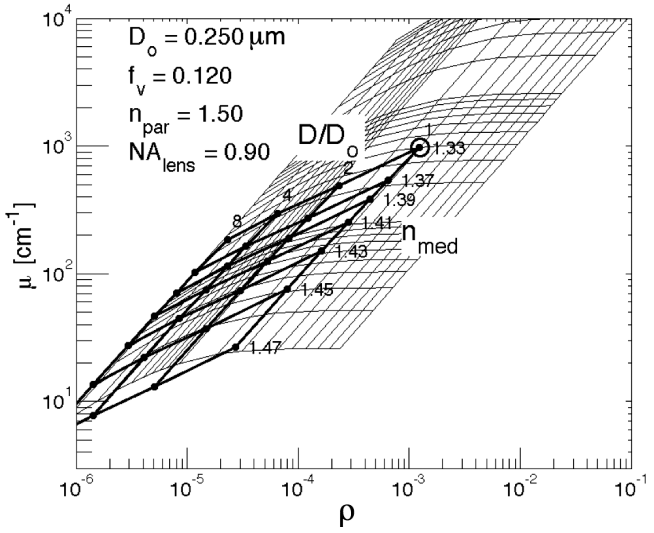

Fig. 5. Mie theory approximation of expected changes in μ, ρ and μ_s, g for a solution of scattering particles, when the refractive index of the medium is changed and the size of the particles is changed. The starting point is an aqueous solution ($n_{\text{med}} = 1.33$) of spherical particles of diameter $D_o = 0.250\,\mu$m, refractive index $n_{\text{par}} = 1.50$, at a concentration of volume fraction $v_f = 0.12$. The wavelength is $0.488\,\mu$m. The numerical aperture of the lens is $NA = 0.90$. The bold lines show a grid where the n_{med} is varied as 1.33, 1.37, 1.39, 1.41, 1.43, 1.45 and 1.47, and the size of the particles is varied as D_o, 2 D_o, $4D_o$ and $8D_o$. This grid illustrates that changing only n_{med} will cause a drop in μ_s but not a change in g. The observed change in the anisotropy of skin scattering caused by glycerin is likely due to an increase in the size of collagen fibers.

Acknowledgment

This work was supported in part by the National Institutes of Health (R01-CA113947, R01-HL084013) in the USA. Kevin G. Phillips was supported by the National Institutes of Health under the Ruth L. Kirschstein National Research Service Award 5-T32-CA106195-05, "Training in the Molecular Basis of Skin Pathobiology," from the National Cancer Institute and the OHSU Cancer Institute, funded by the National Cancer Institute, CA-069533.

References

1. D. S. Gareau, G. Merlino, C. Corless, M. Kulesz-Martin, S. L. Jacques, "Noninvasive imaging of melanoma with reflectance mode confocal scanning laser microscopy in a murine model," *J. Investigat. Dermatol.* **27**(9), 2184–2190 (2007).
2. R. Samatham, S. L. Jacques, P. Campagnola, "Optical properties of mutant versus wild-type mouse skin measured by reflectance-mode confocal scanning laser microscopy (rCSLM)," *J. Biomed. Opt.* **13**, 041309 (2008).
3. K. G. Phillips, R. Samatham, N. Choudhury, G. C. Gladish, P. Thuillier, S. L. Jacques, "*In vivo* measurement of epidermal thickness changes associated with tumor promotion in murine models," *J. Biomed. Opt.* in press (2010).
4. R. K. Wang, X. Xu, V. V. Tuchin, J. B. Elder, "Concurrent enhancement of imaging depth and contrast for optical coherence tomography by hyperosmotic agents," *J. Opt. Soc. Am. B* **18**, 948–953 (2001).
5. S. R. Millon, K. M. Roldan-Perez, K. M. Riching, G. M. Palmer, N. Ramanujam, "Effect of optical clearing agents on the in vivo optical properties of squamous epithelial tissue," *Lasers Surg. Med.* **38**, 920–927 (2006).
6. $n_{80\%DMSO}$ is 1.4523 at 546 nm at 25°C, from R. G. LeBel, D. A. I. Goring, "Density, viscosity, refractive index, and hygroscopicity of mixtures of water and dimethyl sulfoxide," *J. Chem. Eng. Data* **7**(1), 100–101 (1962).
7. $n_{glycerol}$ = 1.4729 at 589.29 nm, from http://en.wikipedia.org/wiki/List_of_refractive_indices.
8. D. S. Gareau, *In Vivo* Confocal Microscopy In Turbid Media, Ph.D. Dissertation, Oregon Health and Science University, Portland, Oregon, USA (2006)
9. S. L. Jacques, D. Levitz, R. Samatham, N. Choudhury, F. Truffer, D. S. Gareau, "Light scattering in confocal reflectance microscopy," Chap. 7 in *Biomedical Applications of Light Scattering*, A. Wax, V. Backman, Eds., McGraw Hill Publishing (2010).